Iraqi Journal of Physics, 2020 *Vol.18, No.45, PP. 76-88*

DOI: 10.20723/ijp.18.45.76-88

Effect depositions parameters on the characteristics of $Ni_{0.5}Co_{0.5}Fe_2O_4$ nanocomposite films prepared by DC reactive magnetron Co-Sputtering technique

Tawfiq S. Mahdi and Firas J. Kadhim

Department of Physics, College of Science, University of Baghdad, Baghdad, Iraq

E-mail: dr.firas90@yahoo.com

Corresponding author: tawfik.s28@gmail.com

Abstract

In this work, spinel ferrites ($NiCoFe_2O_4$) were prepared as thin films by dc reactive dual-magnetron co-sputtering technique. Effects of some operation parameters, such as the distance between electrodes (inter-electrode distance), and preparation conditions such as gas mixing ratio of argon and oxygen, on the structural and spectroscopic characteristics of the prepared samples were studied. For samples prepared at an inter-electrode distance of 5 cm, only one functional group of OH- was observed in the FTIR spectra as all bands belonging to the metal-oxygen vibration were observed. Similarly, the XRD results showed that decreasing the pressure of oxygen in the gas mixture leads to grow more crystal planes in the samples prepared at an inter-electrode distance of 5 cm. The energy band gap was determined for the sample prepared with a mixing ratio of 65:35 and found to be 2.7, 2, and 3.35 eV for direct allowed, direct forbidden, and indirect allowed transitions, respectively. The high structural purity was confirmed as no traces for any elements other than Co, Ni, Fe, and O were found in the final samples.

Keywords

Magnetron sputtering, reactive sputtering, spinel ferrite, thin films

Article info.

Received: Mar. 2020
Accepted: May. 2020
Published: Jun. 2020

تأثير معاملات الترسيب على خصائص أغشية المتراكب ألنانوي $Ni_{0.5}Co_{0.5}Fe_2O_4$ ألمحضرة بواسطة تقنية ألترذيذ ألماكنتروني ألتفاعلي ألمشترك

توفيق صالح مهدي و فراس جواد كاظم

قسم الفيزياء، كلية العلوم، جامعة بغداد، بغداد، العراق

الخلاصة

في هذا البحث، جرى تحضير مركب نيكل-كوبالت فيرايت المغزلي على شكل أغشية رقيقة بواسطة تقنية الترذيذ المشترك الماكنتروني التفاعلي المستمر. تم دراسة تأثير عدد من معاملات التشغيل، مثل المسافة ما بين القطبين وكذلك ظروف التحضير، مثل نسب غازي الآركون والأوكسجين في الخلطة الغازية، على الخصائص التركيبية والطيفية للعينات المحضرة. في العينات المحضرة عند مسافة ما بين القطبين 5cm ظهرت القمم العائدة لاهتزازت جزيئات المركب المطلوب إضافة لقمة وحيدة تعود لمجموعة OH^- كما أظهرت أنماط حيود الأشعة السينية أن تقليل نسبة غازالأوكسجين في الخلطة الغازية أدى لنمو مستويات بلورية أكثرعدداً. جرى تحديد قيمة فجوة الطاقة للعينات المحضرة باستخدام الخلطة الغازية 65:36 وبلغت 2.7 eV للانتقالات المباشرة المسموحة و 2 eV للانتقالات المباشرة غير المسموحة و 3.35 eV للانتقالات غير المباشرة المسموحة. تم تأكيد النقاوة التركيبية العالية للتراكيب المحضرة إذ لم تظهر أية آثار لعناصر أخرى ما عدا الكوبالت والنيكل والحديد والأوكسجين في العينات النهائية.

Introduction

Ferrites are compound of mixed oxides of iron and one or more other materials which have ferrimagnetic properties. Ferrites are regarded as good magnetic materials because of their higher resistivity, low cost, easy manufacturing, and favorable magnetic properties [1]. They are extensively used as permanent magnets, transformer core, high-frequency application, and microwave devices [2]. These compounds have several types based on the crystal structure, like spinel ferrite, garnet ferrite, hexagonal ferrite, and other ferrites [3]. The first type (spinel ferrite) is the class of oxide materials with remarkable electrical and magnetic properties, which have been investigated and applied during the last few decades. Due to their magnetic properties, spinel ferrites have various applications in numerous fields including microwave devices, recording media, magnetic fluids, gas sensors, high-density information storage, ferrofluids, and catalysts [4]. In spinel cubic structured ferrites, MFe_2O_4 (M= Mn^{2+}, Co^{2+}, Ni^{2+}, Zn^{2+}, etc.) here in, oxygen forms face-centered cubic (f.c.c.) closed packing and M^{2+} and Fe^{3+} occupy either tetrahedral (A) or octahedral (B) interstitial sites [5]. The magnetic properties of ferrite nanoparticles also get influenced by the method of synthesis and process parameters even though the common diagnostic tools, such as XRD, show similar crystalline structure [6]. It is known that the magnetic properties depend on the site occupancies by the magnetic ions [7]. Cobalt and nickel, both the ferrites, belong to the category of inverse spinel ferrites. Therefore, by substituting the Co^{2+}, Ni^{2+}, and/or Fe^{3+} ions by suitable cations, their structures undergo a change from inverse spinel to mixed spinel, leading to a corresponding change in the magnetic properties. Thus, by the choice of the cations as well as their distribution in tetrahedral and octahedral sites of the lattice, interesting and useful magnetic properties can be obtained [8]. Following what was mentioned above regarding the various types of ferrite, the composition under research aims to put both Co and Ni together in a stable, usable composition through which soft, high-magnetization alloy is widely used for recording head poles, thin-film inductors or transformers. $NiCoFe_2O_4$ alloys have been demonstrated to have a low coercively and high-saturation magnetization [9]. $NiCoFe_2O_4$ ternary alloys, rich in Fe, have also been noted for their low thermal expansion property, and commercial applications of these alloys include microwave guides, spacecraft optics, laser housings, and printed wired boards [10]. At the same time, the hard facing alloys based on Co or Ni have used for their high mechanical and chemical properties especially their wear and corrosion resistance at high temperatures [11]. Also, $NiCoFe_2O_4$ can be used as a binder with unique properties [12]. This binder when subjected to plastic deformation, it substantially maintains its face-centered cubic (f.c.c.) crystal structure and avoids stress and/or strain-induced transformations [13]. Cobalt ferrite ($CoFe_2O_4$) is a well-known hard magnetic material with high coercively and moderate magnetization, which is useful in high-density digital recording discs and audio/videotape. However, $CoFe_2O_4$ has a high magneto crystalline anisotropy, which makes it difficult to achieve high initial susceptibility or magnetic conductivity [14], while nickel ferrite ($NiFe_2O_4$) is a typical soft magnetic material with lower magneto crystalline anisotropy [15]. It provides an effective way to reduce the

anisotropy of $CoFe_2O_4$ by partly substituting Co^{2+} for Ni^{2+}, $NiCoFe_2O_4$. In view of the above, a new type of nanocomposite, $NiCoFe_2O_4$, which has controllable magnetic properties, is expected to be used in electromagnetic and nanotechnology applications. Amongst all inverse spinel ferrites, the nickel substituted cobalt ferrite has been extensively studied in view of their good chemical and thermal stability, high electrical resistivity, magnetic anisotropy, high coercivity, and moderate saturation magnetization, various exchange interactions and super-paramagnetism, etc. In addition, they exhibit ferrimagnetism, originating from the magnetic moment of anti-parallel spins between Fe^{3+} ions at tetrahedral sites and Co^{2+} or Ni^{2+} ions at octahedral sites [16].

Co-sputtering of materials offers an important alternative to complex and sometimes impossible alloying of metallic materials for a single sputtering target [17, 18]. Up to now, co-sputtering was accomplished with either two small, usually round cathodes [19, 20] or a multicomponent, tailored target [21].

Experimental part

Spinal ferrites thin films were deposited onto glass substrate using lab-made dc reactive closed-field unbalanced dual magnetron (CFUBDM) co-sputtering technique. A high purity cobalt and nickel (99.99%) targets were mounted on the cathode according to a geometrical arrangement. The geometrical arrangement shown in Fig.1 was proposed according to a numerical treatment carried out to determine the dimensions of both sheets with respect to each other to achieve the required doping process. This numerical treatment was performed by applied Modeling Lab. at using Q-point Software produced by TimX Company, Japan. Both electrodes (cathode and anode) were made of stainless steel with 10 cm diameter and 4 mm thickness which were placed parallel to each other and the anode could be vertically moved to adjust the distance between target and substrate. The electrodes were connected to dc power supply to provide the required electric power. The plasma was generated by the electric discharge of argon gas while the oxygen gas with a purity of 99.99% was used as a reactive gas. The mixing ratio of both gases was controlled using a stainless steel mixer before and flowed into the deposition chamber. The deposition chamber was evacuated to base pressure about $2x10^{-2}$ mbar by an Edward double-stage rotary pump with a suction power of 8 m^3/hr to reduce uncontrolled contamination during the experiment to minimum concentration. The pressure during the operation was kept to a constant value of approximately $5x10^{-2}$ mbar, several gas mixing ratios were used for each inter-electrode distance. When the inter-electrode distance is 4 cm, gas mixing ratios Ar:O_2 were 50:50, 60:40, 75:25 and 80:20 while the mixing ratios were 50:50, 55:45, 60:40, and 65:35 for inter-electrode distance of 5 cm. Crystallographic and the optical characteristics of the prepared samples were determined by the Fourier-transform (FTIR), standard x-ray diffraction (XRD) analysis, Scanning electron microscopy (SEM), Energy Dispersive X-ray Diffraction (EDX), and UV-Visible spectroscopic. The final samples presented in this work were prepared without heat treatment of the cathode and the anode for 2 hours of deposit time.

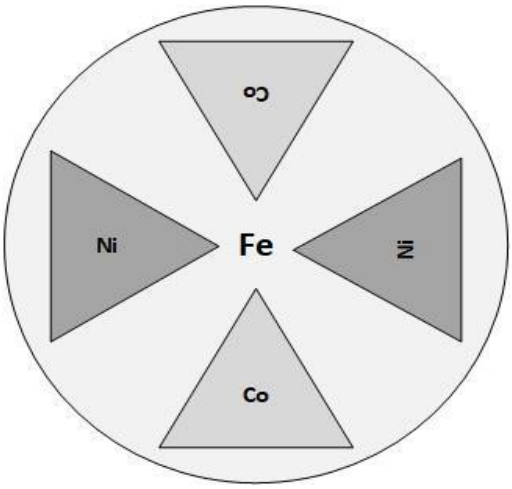

Fig.1: Geometrical arrangement of the co-sputtering using Ni, Co, and Fe target.

Results and discussion

The FTIR spectra recorded in the range of 400-4000 cm^{-1} are shown in Fig.2. The bands of solids are usually assigned to the vibration of ions in the crystal lattice. There are two main frequency bands, namely, the high-frequency band (ν_1) is observed at 584 cm^{-1} to 610 cm^{-1} whereas the lower frequency band (ν_2) is observed at 412 to 418 cm^{-1} [22]. These two observed bands ν_1 and ν_2 correspond to the intrinsic vibrations of tetrahedral and octahedral complexes, respectively, following the main characteristics of all the ferrite material [23]. The broad metal-oxygen (M-O) bands are observed in the infrared spectra of samples with a gas mixing ratio (50:50, 60:40, 75:25, and 80:20). The band (ν^1) in 600–550 cm^{-1} region which seen in all gas mix ratio samples were detected due to tetrahedral metal-oxygen ($CoFe_2O_4$, $NiFe_2O_4$) stretching vibration [23]. The absence of obvious peak that due octahedral coordinated metal ions had been noticed and that an indication to lower frequency band (ν_2) expected to be around 400 cm^{-1} only in gas mix ratio (80:20) where observed at 412-450 cm^{-1}. This probably caused by the broadening of this peak attributed to very small particles of spinel ferrites [24].

From that point in contrast of the samples prepared at different gas mixing ratios (50:50, 55:45, 60:40, 65:35) and 5 cm the inter-electrode distance, as shown in Fig.3, and that lead to the clear observation of the broad metal-oxygen ($CoFe_2O_4$, $NiFe_2O_4$) bands at 400-477 cm^{-1}, 508-604 cm^{-1} excepted in the gas mixing ratio (50:50) on the other side the characteristics of vibrational bands of ($NiCoFe_2O_4$) composite are found in the FTIR spectra located around 508 cm^{-1}, 1368 cm^{-1}, and 1638 cm^{-1} in the sample with gas mix ratio (65:35). From all that has been mentioned above, the two strong bands can be recognized. The first one is around 1638 cm^{-1} attributed to the bending vibrations of (O-H) band which also is overlapping with that in ($NiCoFe_2O_4$) composite, while the second-wide band peak at 3451 cm^{-1} s is assigned to the stretching modes of the free or adsorbed water vapor. This adsorption has resulted during the testing process as the deposition process was confirmed by the XRD patterns to produce highly-pure structures [25].

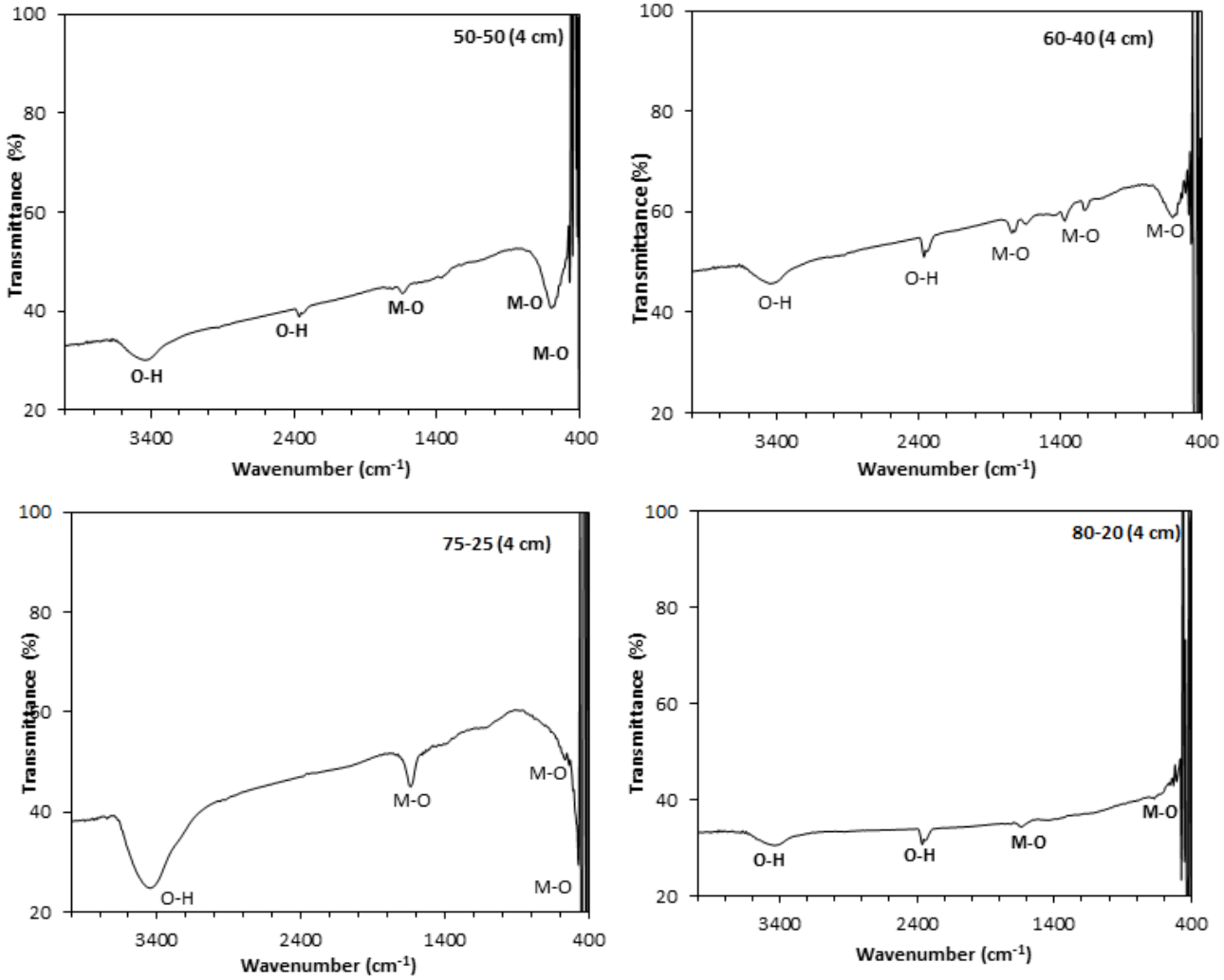

Fig.2: FTIR spectra for samples prepared at inter-electrode distance of 4 cm.

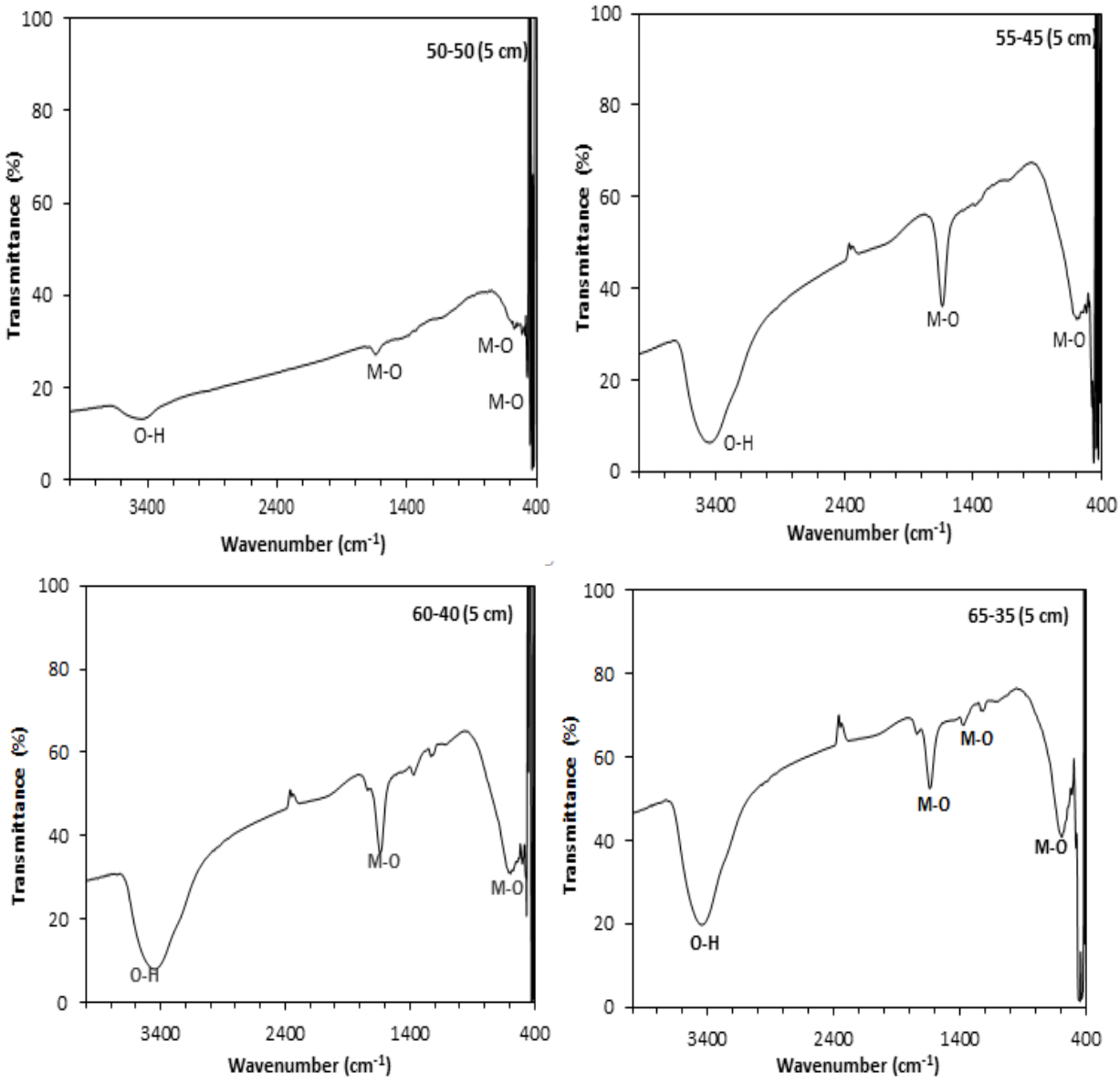

Fig.3: FTIR spectra for samples prepared at inter-electrode distance of 5 cm.

Using both inter-electrode distances (4 and 5) cm and several gas mixing ratios, the spinel structures were observed in the XRD patterns, as shown in Figs. 4 and 5. The XRD analysis of sample prepared at inter-electrode distance of 4 cm and gas mixing ratios Ar:O_2 of 50:50 and 60:40 showed the presence of six characteristic peaks at 30.32°, 35.60°, 37.06°,43.22°, 53.76°, and 57.48°. These peaks are corresponding to Miller indices (220), (311), (222), (400), (422), and (510), respectively for the spinel α-ferrite [26]. This confirms the formation of spinel simple cubic structure (JCPDS, No. 86-2267, Fd-3m) while the samples prepared using mixing ratios of 75:25 and 80:20, there was no evidence on the formation of spinel structure except CoF_2O_4, which was observed in the sample prepared using mixing ratio of 75:25 without the formation of NiF_2O_4. This can be attributed to the fact that the Ni^{2+} ion (radius of 0.78Å) is smaller than Co^{2+} ion (radius of 0.82Å) [27]. On the other hand, the samples prepared at inter-electrode distance of 5 cm with mixing ratios of 50:50, 55:45, 60:40, and 65:35 showed all peaks assigned to the formation of spinel α-ferrite, in addition to the $NiCoF_2O_4$ as single-phase cubic spinel structure, especially for mixing ratio of 65:35, as confirmed by JCPDS card (1-1221). No peaks of impurities could be observed, which confirms the high purity of prepared samples. The average grain size of the composite was estimated using Debye-Scherer's equation [28]

$$D = \frac{0.89\lambda}{\beta \cos\theta} \quad (1)$$

where D is the grain size, 0.89 is the Scherrer's constant, λ is the x-ray wavelength, β is the full-width at half maximum (FWHM) and θ is the corresponding Bragg's angle. The average grain size of the sample prepared with a mixing ratio of 65:35 was found to be 14.43 nm.

The scanning electron microscopic image of all the synthesized samples was shown in Fig.6. The images show that the particles have an almost homogeneous distribution, and some of them are in agglomerated form. Also the micrographs show the presence of a number of interfaces. It is evidenced by SEM images that the aggregation of particles lies in the nanometric region. The average grain size for the prepared sample varies from 26.86 nm to 40.82 nm. It was noted that the average grain size of the samples obtained from SEM images is larger than nanocrystal size calculated from the XRD measurements, which indicates that each grain is formed by aggregation of a number of nanocrystals. The shape of the formed nanoparticles could not be determined due to the limited resolution of the measuring instrument to 200nm. The particles were observed as uniform grains (in different SEM images) confirming the crystalline structure of Ni-Co ferrite which were detected by XRD studies.

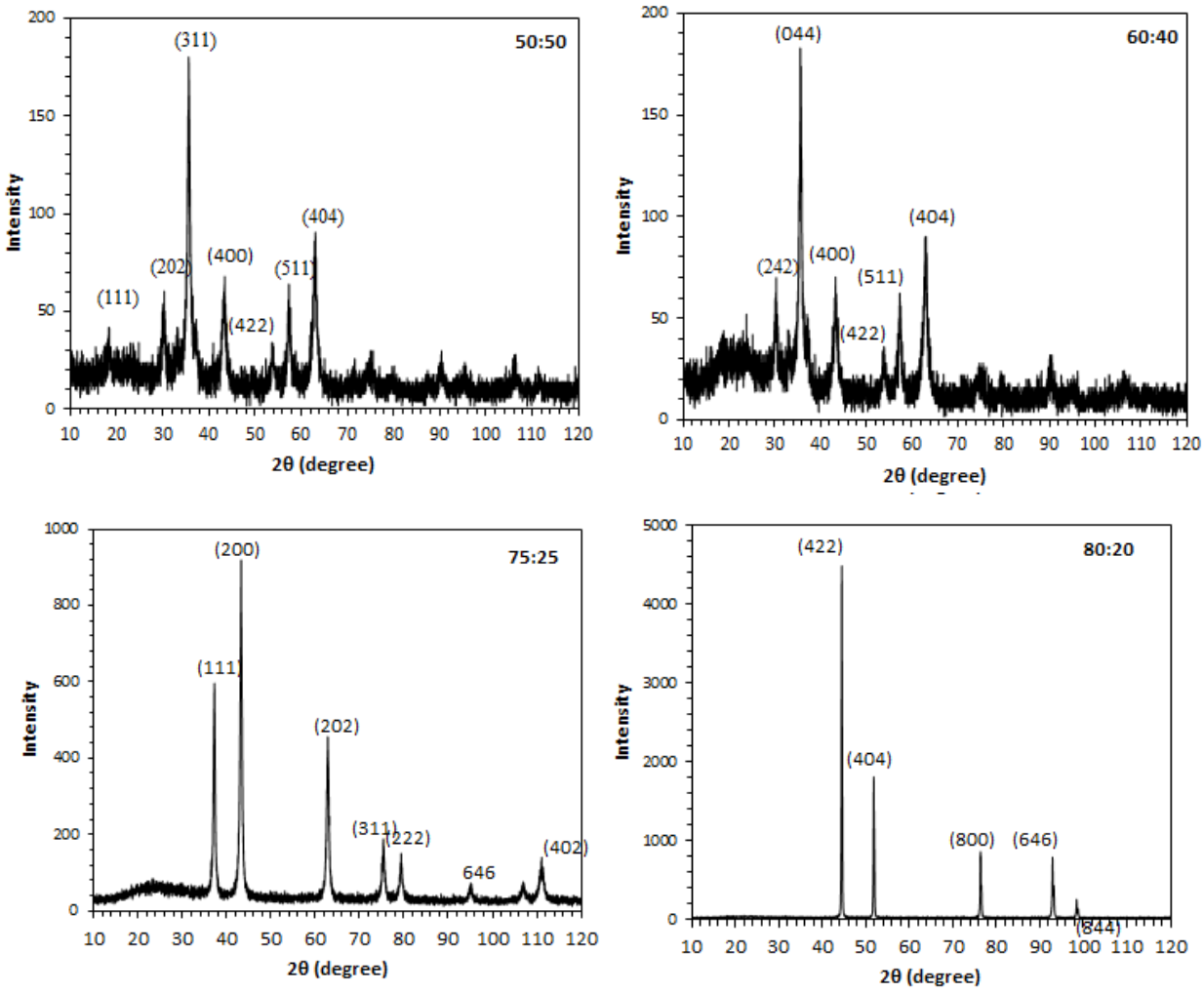

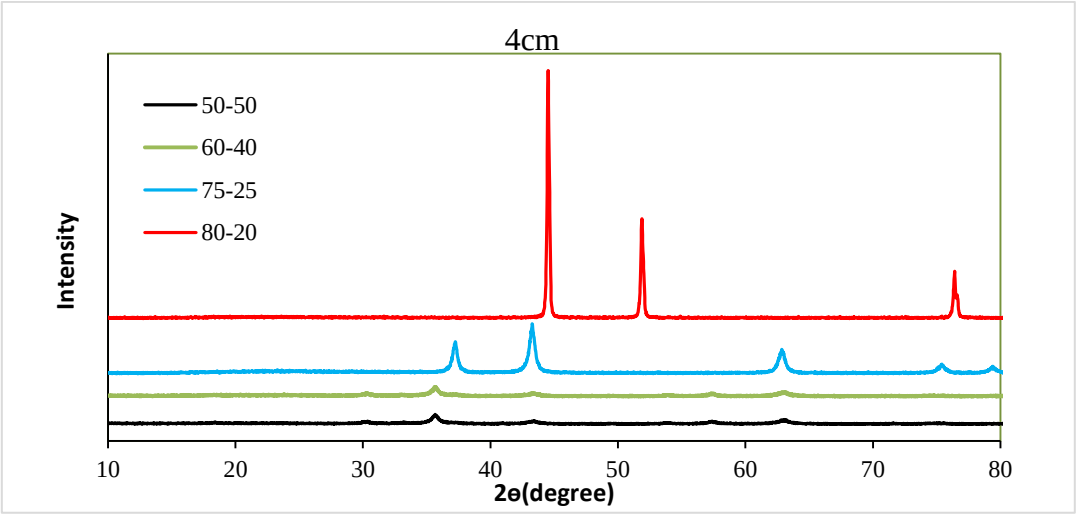

Fig.4: X-ray diffraction (XRD) of samples prepared at inter-electrode distance of 4 cm

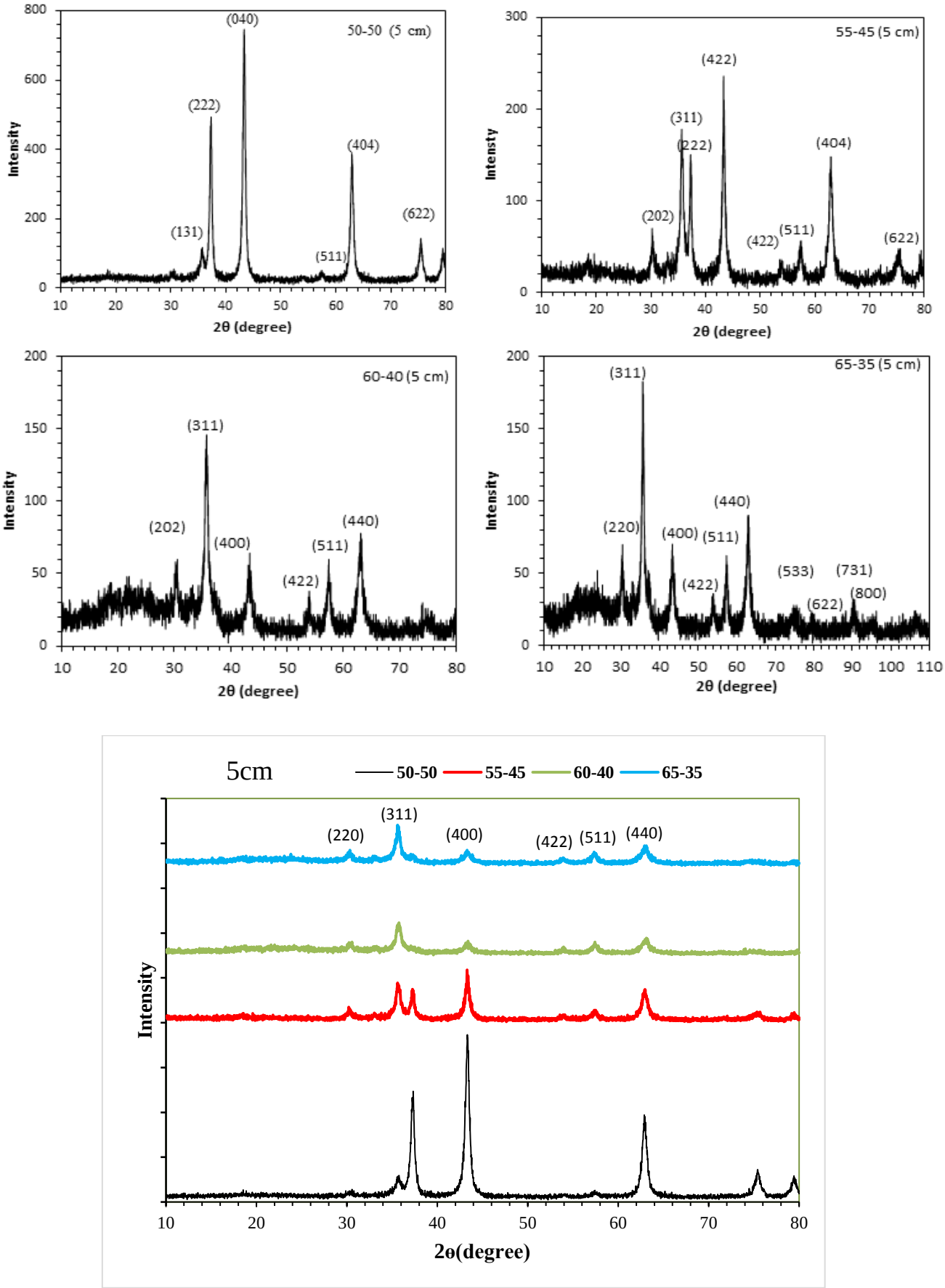

Fig.5: X-ray diffraction (XRD) of samples prepared at inter-electrode distance of 5 cm.

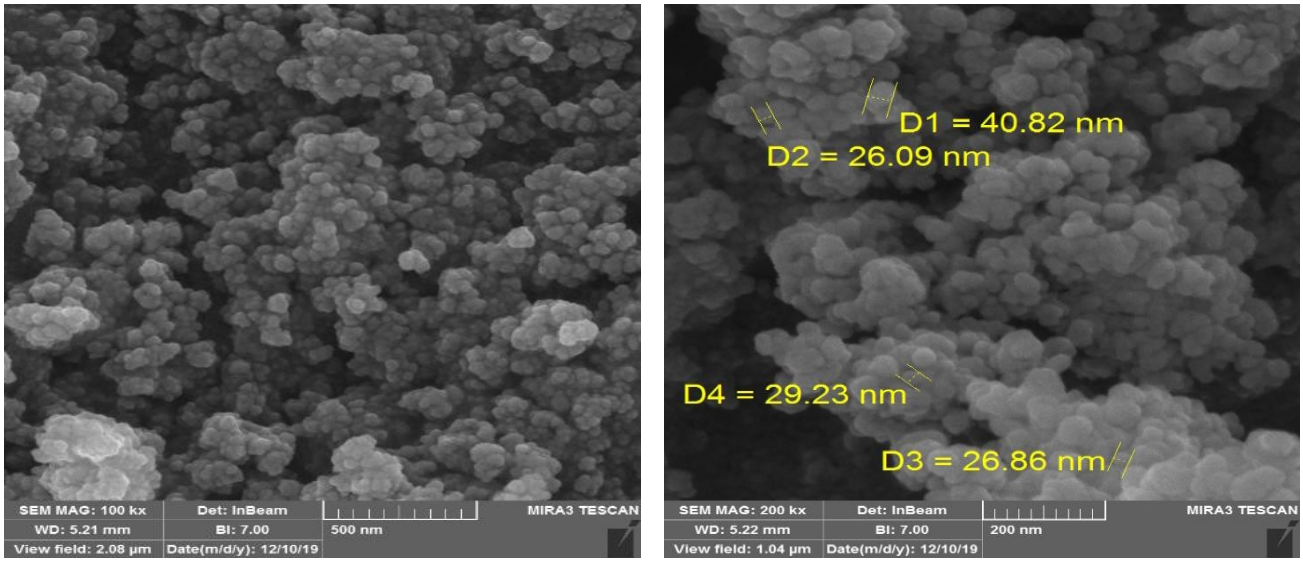

Fig.6: SEM of the nanostructured NiCoFe2O4 thin film prepared using Ar: O_2 gas mixture of 65:35.

The EDX is an analytical technique used for the elemental analysis or chemical characterization of the prepared sample. It relies on interaction of x-ray excitation and a solid sample. Its characterization capabilities are due in large part to the fundamental principle that each element has a unique atomic structure allowing a unique set of peaks on its electromagnetic emission spectrum. It was essential to check the chemical composition of the sample, so the required compound ($Ni_{0.5}Co_{0.5}Fe_2O_4$) prepared with a gas mixing ratio ($Ar:O_2$) of 65:35 and inter-electrode distance of 5 cm was confirmed by EDX. The qualitative composition of the prepared samples as well as the quantitative presence of Co, Ni, Fe, and O in these samples are presented in Fig.7 and the percentage elemental and atomic amounts of these elements are given in Table1. This result confirms the stoichiometry of the prepared compound. Also, no trace of any impurity was found in the EDX spectrum which confirms the high structural purity of the synthesized material.

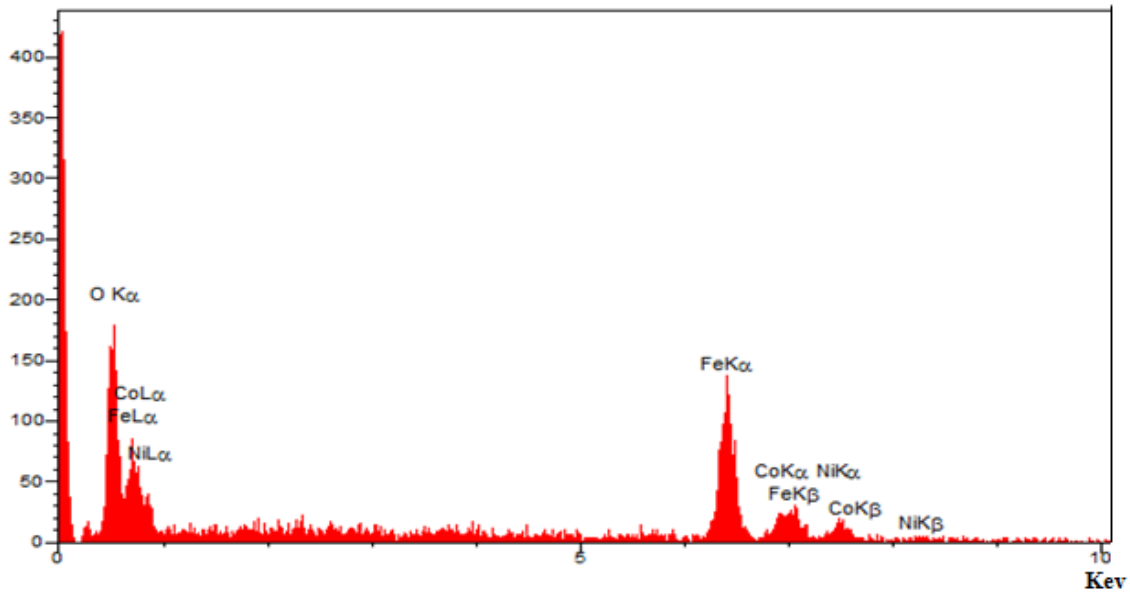

Fig.7: EDX result of $NiFe_2O_4$ sample prepared using $Ar:O_2$ gas mixture of 65:35.

Table1: Element of each sample composition Ni-Co ferrite analyses by (%weight).

$NiCoFe_2O_4$ Composite	Ni	Co	Fe	O	Sum
wt. %	8.26	9.93	53.25	28.57	100%
A %	4.61	5.53	31.28	58.58	100%
B.E	4.47	4.43	4.34		

The reactive dc dual-magnetron sputtering technique is a convenient way for obtaining a homogeneous tiny spinel ferrite (Ni ferrite, Co ferrite) and mixed spinel ferrites. The process involves no impurity pickup or material loss.

The absorption spectra of the prepared samples were recorded in the spectral range of 300-800 nm at room temperature as illustrated in Fig.8. The absorbance increases with increasing of argon pressure in the gas mixture (i.e., decreasing oxygen pressure) and this behavior is similar to that of samples prepared at different conditions, such as inter-electrode distance of 5 cm, and gas mixing ratio of 50:50, 55:45, 60:40, and 65:35 after the same deposition time. This increase in absorbance agrees to Beer-Lambert law as longer deposition time leads to increase film thickness, which represents the sample length in the law.

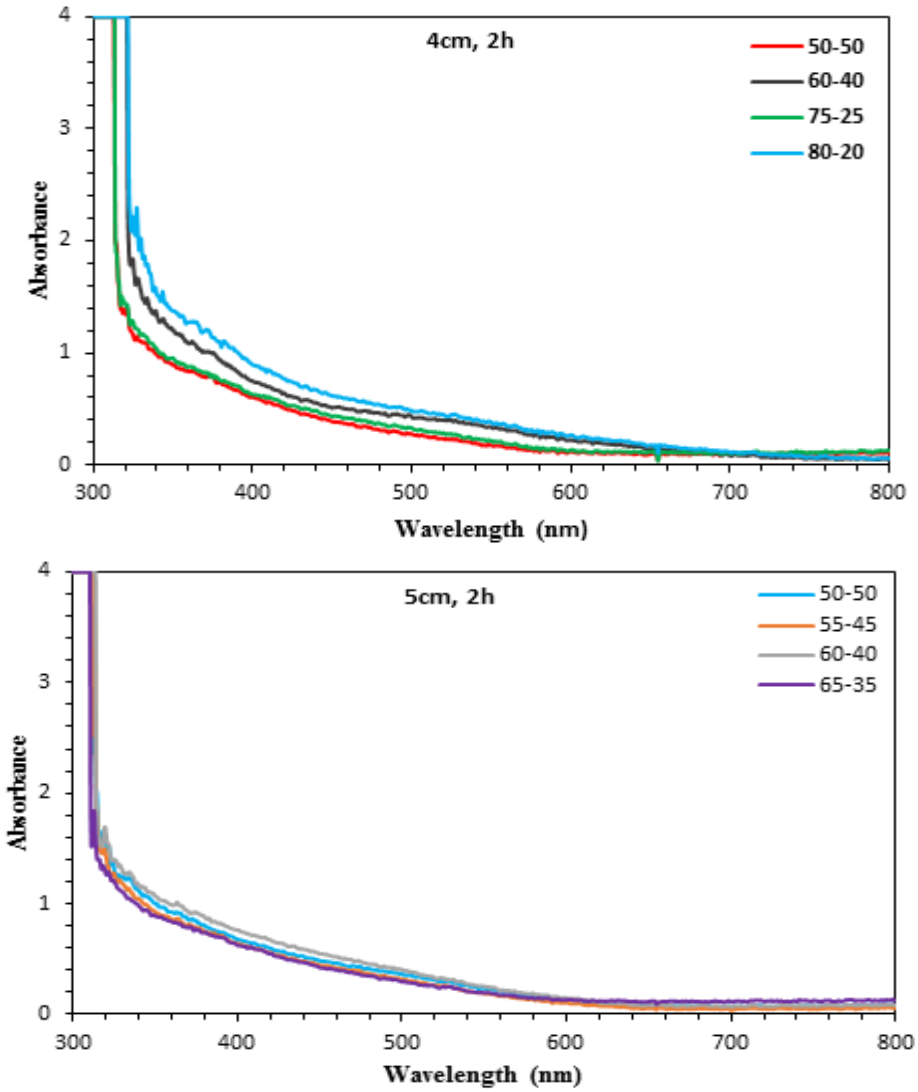

Fig.8: Absorption spectra of prepared samples of thin film using different gas mixing ratios and different deposition time at two inter-electrode distances (4cm and 5cm).

From the last figures, the prepared samples exhibit high absorption at the spectral region shorter than 300 nm and an absorption edge at about 320 nm. The energy bandgap of the ternary ($NiCoF_2O_4$) sample prepared with the mixing ratio of (65:35) can be calculated by:

$$\alpha = \frac{A(h\upsilon - E_g)^n}{h\upsilon} \quad (2)$$

where α is the absorption coefficient, E_g is the energy band gap, A is constant, and n is a given value depends on the nature of the optical transition (allowed direct, allowed indirect, forbidden direct, or forbidden indirect). The intercept of linear behavior of $(\alpha h\nu)^2$, $(\alpha h\nu)^{1/2}$ and $(\alpha h\nu)^{3/2}$ versus $h\nu$ assigns that the direct (allowed and forbidden) and indirect transitions, respectively, are the dominant as shown in Fig.9 and determines the energy band gap of the prepared material [29].

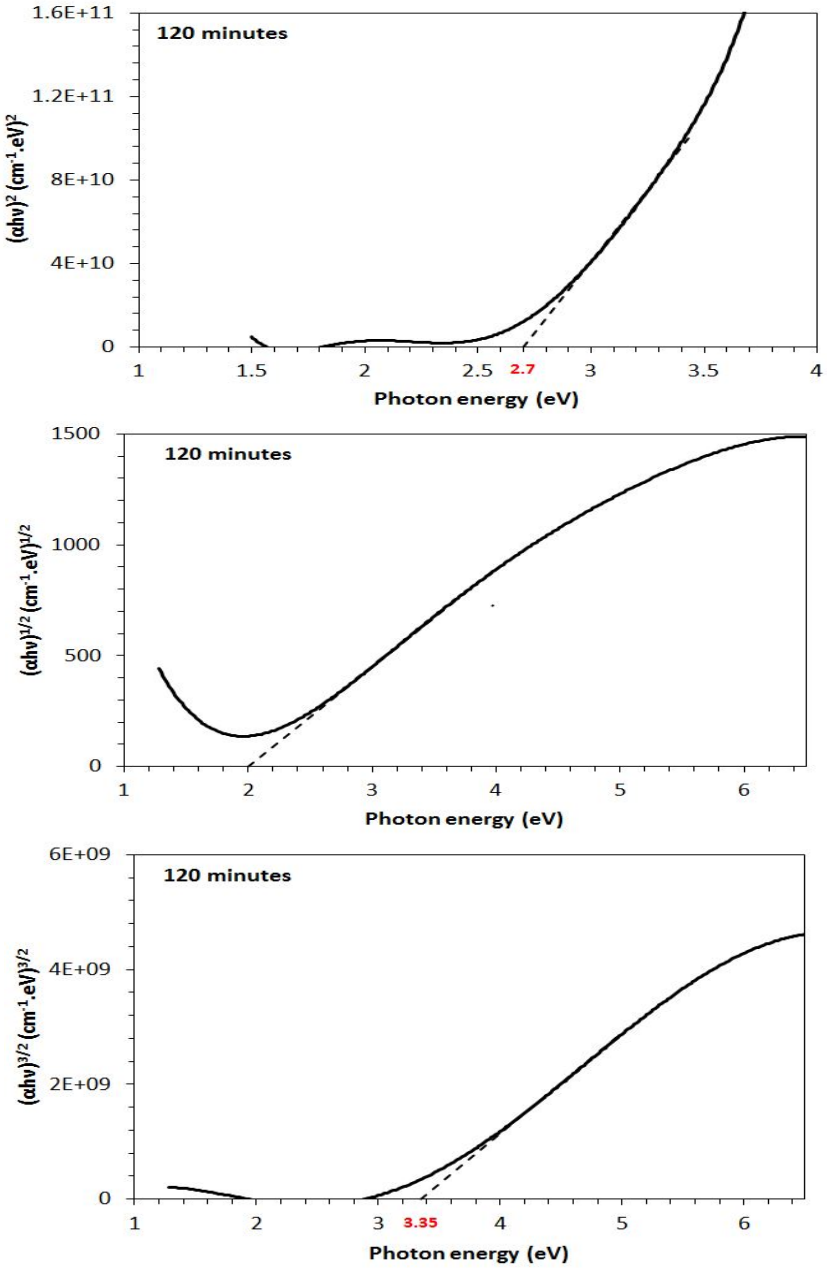

Fig.9: Determination of indirect energy band gap for ($NiCoF_2O_4$) samples prepared using gas mixture ratio 65:35 (a) indirect transition and (b) direct transition.

Conclusions

Highly-pure spinel ferrites ($Ni_{0.5}Co_{0.5}Fe_2O_4$) were synthesized by the dc reactive magnetron co-sputtering technique. The high structural purity of the prepared samples was confirmed by the characterization as no impurities were found in the final sample. The fine control of the structural compositions could be performed by controlling both operation parameters and preparation conditions of the co-sputtering system.

References

[1] C. Barry Carter, M. Grant Norton, Ceramic Materials, Science and Engineering, Springer, New York, (2007) 212-215.
[2] G. Catalan, Adv. Mater., 21 (2009) 2463-2485.
[3] X. Liu, P.H. Gomez, S. Zhou, J. Magn. Magn. Mater., 305 (2006) 524-528.
[4] M.J. Iqbal and Z. Ahmad, J. Appl. Phys., 111 (2012) 033906-033907.
[5] J. Philip, G. Gnanaprakash, G. Panneerselvam, M.P. Antony, T. Jayakumar, B. Raj, J. Appl. Phys. 102 (2005) 054305-054306.
[6] M. Sugimoto, J. Am. Ceram. Soc., 82, 2 (1999) 269-280.
[7] A.S Albuquerque, J.D Ardisson, W.A.A Macedo, J. Magn. Magn. Mater., 226-230, Pt. 2 (2001) 1379-1381.
[8] K. Rajasekhar Babu, K. Rama Rao, B. Rajesh Babu, J. Magn. Magn. Mater., 434 (2017) 118-125.
[9] T. Osaka, M. Takai, K. Hayashi, K. Ohashi, M. Saito and K. Yamada. Nature, 392 (1998) 796-798.
[10] N.H. Phan, M. Schwarz, K. Nobe, J. Am. Electroplat. Soc., 75 (1988) 44-48.
[11] U. Malayoglu and A. Neville. J. Wear, 259 (2005) 219-229.
[12] M. Bahgat, Min-Kyu Paek, Chul-Hwan Park and Jong-Jin Pak. Mater. Trans., 49, 1 (2008) 208-214.
[13] X. Liu, J. O. Rantschler, C. Alexander, G. Zangari. J. IEEE Trans. Magnet., 39 (2003) 2362-2364.
[14] V. Pallai, D.O. Shah. J. Magn. Magn. Mater., 163 (1996) 243-248.
[15] L.G. van Uitert. J. Chem. Phys., 24 (1956) 306-310.
[16] R.C. Kambale, P.A. Shaikh, S.S. Kamble, Y.D. Kolekar, J. Alloys and Compounds, 478 (2009) 599-603.
[17] W.R. Sinclair and F.G. Peters, Rev. Sci. Instr., 33 (1962) 744-746.
[18] A. Belkinda R. Lairdb Z. Orbanc P. White Rafalkoc, Thin Solid Films, 219, (1-2) (1992) 46-51.
[19] H. Guo, Y. Li, Xiang Fang, K. Zhang, J. Ding, N. Yuan. Mater. Lett., 162 (2016) 97-100.
[20] C. Misiano and E. Simonetti. Vacuum, 27, 4 (1977) 403-406.
[21] J. Felts and M. McBride, Society of Vacuum Coaters, 34th Annual Technical Conference Proceedings, (1991) 235-239.
[22] T. Ramesh, S.Senthil Kumar, R.S. Shinde, S.R. Murthy. J. Solid State Physics, 345 (2015) 130046-1_130046-3.
[23] R.D. Waldron. Phys. Rev., 99 (1955) 1727-1735.
[24] B. Smith, "Infrared Spectra Interpretation A Systematic Approach", CRC Press, New York, (1998), p. 288.
[25] S. Prabahar and M. Dhanam, J. Cryst. Growth, 285(1-2) (2005) 41-48.
[26] L. Vegard, *Zeitsch rift fiir Physics*, 5(17) (1921) 17-23.
[27] M. Freitasa, G. Gouveiaa, L. Costab, A. Oliveirab, R. Kiminami. Mater. Res., 19 (Suppl. 1) (2016) 27-32.
[28] S. Qiu, S.J. Kalita. Mater. Sci. Eng., A 435–436 (2006) 327-332.
[29] S.S. Nair, M. Mathews, M.R. Anantharaman Chem. Phys. Lett., 406 (2005) 398-403.